Chemical Engineering Journal 165 (2010) 701–708

Contents lists available at ScienceDirect

Chemical Engineering Journal

journal homepage: www.elsevier.com/locate/cej

Novel binderless zeolite-coated monolith reactor for environmental applications

Juan M. Zamaro*, Eduardo E. Miró

Instituto de Investigaciones en Catálisis y Petroquímica, INCAPE (FIQ, UNL-CONICET), Santiago del Estero 2829, 3000 Santa Fe, Argentina

ARTICLE INFO

Article history:
Received 10 April 2010
Received in revised form 4 October 2010
Accepted 7 October 2010

Keywords:
Zeolite
Monolith
Hybrid properties
Binderless coating
SCR of NO_x

ABSTRACT

A novel structured catalyst based on a binderless zeolite film was developed onto a cordierite monolith. The zeolitic film was obtained performing a binderless washcoating which was followed by a hydrothermal treatment, which resulted in a coating with hybrid physicochemical properties, having a porous washcoat-like microstructure with an intergrowth between the aggregates. This combination confers to the zeolite coating an open structure which is an advantage of washcoats and a high mechanical stability characteristic of the zeolite growths. It should be emphasized that these desired properties are obtained without the use of binders. The physico-chemical properties were investigated through MIP (mercury intrusion porosimetry), SEM (scanning electron microscopy), ultrasonic adherence tests, NO-TPD (temperature-programmed desorption of NO) and EPMA (electron probe microanalysis). The catalytic properties of the monolith were evaluated in the selective catalytic reduction of NO_x at high spatial velocities, showing promising results.

1. Introduction

The use of structured catalysts is necessary when high flow rates of dusty gases are to be treated, as in the case of the catalytic treatment of gases from combustion processes. In these applications, low pressure drop and good tolerance to plugging by dust are essential requisites leading to the use of open catalytic structures [1]. Cordierite honeycomb monoliths were initially developed for the automotive industry [2] and, in view of its excellent physicochemical properties, it has become one of the most widely used structured supports to be employed in environmental catalytic applications.

On the other hand, zeolite coatings are attractive to be used as catalyts due to their broad range of properties which make them highly versatile for several catalytic reactions. In this sense, zeolite-coated cordierite monoliths have been successfully evaluated in environmental catalytic applications such as in the selective catalytic reduction (SCR) of NO_x with ammonia in stationary sources [3] or with hydrocarbons under lean conditions in mobile sources [4–6]. Moreover, zeolitic cordierite monoliths have been studied for other than environmental applications as in the production of chemicals [7–9].

In order to obtain a zeolite film onto a cordierite monolith, there are two main ways: by hydrothermal synthesis or by deposition of particles from a slurry (washcoating). The first method involves growth and intergrowth processes of crystals onto the cordierite monolith walls. Through this method, it was possible to obtain stable in situ zeolite-coated cordierite monoliths [10–14] which were later successfully employed in catalytic reactions [15,16]. However, in many cases the zeolite synthesis on cordierite walls could leave a compact structure of the coating when high crystalline intergrowth and crystals overgrowth on the surface take place [17]. This could cause diffusive restrictions in the coating and therefore it is desirable to obtain a non-dense porous film, but having high mechanical stability.

Besides, the washcoating method is convenient because highly porous coatings can be obtained. Through this method fairly stable zeolite coatings on cordierite monoliths were obtained, in which the catalytic properties of the powder catalysts were maintained [18]. However, a disadvantage of this method is that an improvement of the mechanical stability of the coatings is needed. To this date, the only way in which this feature has been addressed is through the addition of binders, which are generally nano-sized particles such as SiO_2 [3,7,8,18–20], Al_2O_3 [4,21,22] or aluminum solutions [23,24]. Recently, MFI zeolite washcoats were deposited over micron-sized channeled Fecralloy monoliths, being necessary to add 6 wt.% of silica binder plus 6 wt.% of polyvinyl alcohol to obtain homogeneous and stable washcoats [25]. In another recent work, Cu/ZSM5 washcoats were stabilized with the addition of an amount of 10 wt.% of silica binder [26]. While in some cases these binders might have no prejudicial effect [18] or even be beneficial in the catalytic performance [19], in most cases they lead to a decrease in catalytic activity or selectivity due to a blockage or inactivation of active sites [23], or to the dilution of the active phase. Moreover, their benefit o detriment could depend on whether the reactant flow is wet or dry [20]. For these reasons, it is still challenging to

* Corresponding author. Tel.: +54 342 4536861; fax: +54 342 4536861.
E-mail address: zamaro@fiq.unl.edu.ar (J.M. Zamaro).

1385-8947/$ – see front matter © 2010 Elsevier B.V. All rights reserved.
doi:10.1016/j.cej.2010.10.014

produce zeolite catalytic coatings with porous properties, presenting high mechanical resistance without employing agglomerating substances and being capable of supporting the adverse conditions, characteristics of environmental applications.

We believe that a combination of the two methods, washcoating and synthesis, could result in a coating sharing the advantageous properties of both. The washcoating method can provide the porous properties of the film while a subsequent hydrothermal treatment could bring an intergrowth of the deposited aggregates. In this work, we present the preparation of a catalytic zeolite coating onto cordierite monolith through the combination of the methods mentioned above. The active coating produced has a porous washcoat-like microstructure with an exceptionally high mechanical stability without the use of binders, providing a new alternative to the preparation of binderless and stable catalytic zeolite coatings. The coating thus obtained has hybrid properties (we refer to this as HM) since it exhibits porosity, adherence, microstructure and catalytic behavior different from those coatings that can be obtained using either method individually.

2. Experimental

2.1. Preparation of the monolith reactor

2.1.1. Washcoating of zeolite particles

A portion of cordierite honeycomb monolith of 1 cm × 1 cm of section and 2 cm long containing 64 channels (Corning, 400 cps, 0.17 mm average wall thickness) was used as substrate. The monolith was washcoated with an aqueous suspension of 30 wt.% of NH_4–mordenite powder from zeolyst (Si/Al = 10). The outer faces were covered so that the depositions were performed only inside the channels and after the immersion, the suspension excess was blown. This process was performed twice, and after that the zeolite-coated monolith was dried in a stove at 120 °C. Then, in order to pre-stabilize the coating, the monolith was treated in an oven at 550 °C for 4 h. This later treatment was necessary to prevent the aggregates from becoming detached when subsequently submerging the monolith into the synthesis solution.

2.1.2. Hydrothermal treatment

The calcined washcoated monolith was subjected to a hydrothermal treatment with a reactant mixture with the composition of H_2O:SiO_2:Na_2O:Al_2O_3 = 72:1:0.38:0.025 [15]. The reactants were colloidal SiO_2 (Ludox AS 40), $Na_2Al_2O_4$ (Riedel-de-Häen) and NaOH (Cicarelli pro-analysis) that were aged by stirring for 24 h at r.t. The treatment was conducted at 180 °C for 24 h, placing the monolith with the channels in vertical position fixed inside a Teflon vessel together with the aged synthesis gel. The vessel was transferred to an autoclave which was then placed in a stove for the hydrothermal treatment. After that, the vessel was cooled and the sample was withdrawn from the autoclave, washed in water, and finally dried at 120 °C for 4 h.

2.1.3. Monolith reactor activation

The obtained monolith was first exchanged with ammonium (80 °C, NO_3NH_4 1 M, 24 h) in order to transform the Na–mordenite into NH_4–mordenite, and was then activated through indium incorporation. The NH_4–mordenite monolith was immersed in a 5 wt.% solution of $In(NO_3)_3$ ($(NO_3)_3In{\cdot}5H_2O$ Aldrich) and the excess was blown, repeating this process until obtaining a 4 wt.% of indium, with respect to the zeolite mass. Between blowing steps, the monolith was subsequently dried in a microwave oven and in a stove to obtain more uniform distributions of the indium precursor. Then it was treated at 500 °C in air flow for 12 h to generate the In_2O_3 oxides and decompose the NH_4–zeolite in H–zeolite. Immediately after, the temperature treatment was increased up to 700 °C and maintained for 2 h in order to develop the $(InO)^+$ active sites through solid-state reaction between In_2O_3 and zeolite protons.

2.2. Characterizations

The morphological characteristics of the monolith were determined by scanning electron microscopy (SEM) with a Jeol JSM-35C instrument, operated at 20 kV acceleration voltages. The sample was glued to the sample holder with Ag painting and then, due to the low electrical conductivity of the zeolite and the cordierite, it was coated with a thin layer of Au which resulted in improved images.

The porous structure of the monolith was studied by means of mercury intrusion porosimetry (MIP) technique using a Micromeritics Autopore 9220 V1.04 equipment that was operated from an initial pressure of 1.5 psi up to a final pressure of 50,000 psi, with an equilibration time of 10 s between points. For the pore size calculations, a surface tension of Hg γ = 485 din/cm and a contact angle of θ = 130° were considered.

The mechanical stability of the coating was evaluated through an accelerated test employed in a previous work [18], which consists in the measurement of zeolite weight loss and coating damage caused by exposing the sample to ultrasonic cavitation. The zeolitic monolith was immersed in water inside a glass vessel and then in an ultrasonic bath (Cole Parmer, 47 kHz and 130 W) for 1 h at 25 °C. The weight of the sample both before and after the ultrasonic treatment was measured. The test was complemented by optical microscopic observations, evaluating the physical integrity of the coating after the treatment.

Temperature-programmed desorption of nitric oxide (NO-TPD) was performed on the In-exchanged monolith. The monolith was placed in a quartz reactor heated with a furnace with a temperature controller in a He flow at 400 °C for 2 h in order to perform a surface cleaning; then, it was cooled to r.t. in dry He flow and immediately afterwards put in contact with NO diluted in He (5000 ppm) for 20 min. Then, NO was purged from the gas phase and the temperature-programmed desorption was started at an average heating rate of 10 °C min^{-1}, measuring the gas concentration (NO_x) at the outlet of the reactor with a FTIR instrument Mattson Genesis II equipped with an on-line cell with CaF_2 windows for gas phase analysis. The measurements were carried out taking successive spectra every 2 min during the temperature ramp.

The elemental composition of the coating was obtained performing electron probe microanalysis (EPMA) in a transversal section of the monolith at different locations from the cordierite support to the coating surface (zones 1, 2 and 3 in Fig. 1b, respectively). The X-ray spectra were processed in order to draw the compositional profile. The semiquantitative proportions of the elements were obtained by means of the SEMIQ method.

2.3. Catalytic evaluation

The monolith was tested in the selective catalytic reduction of NO_x with methane in a continuous flow system. The composition of the reacting stream was 1000 ppm NO, 1000 ppm CH_4, and 10% O_2, in He balance. The reaction was performed at temperatures between 300 °C and 650 °C at a 500 cm^3 min^{-1} g $zeolite^{-1}$ total flow/zeolite loading ratio. The monolith was placed inside a quartz reactor between quartz wool plugs, and the free space between the sample and the quartz tube was filled with CSi particles to avoid bypass flow. NO_x and CH_4 conversions were calculated as: $X_A = \frac{[A]^0 - [A]}{[A]^0} \times 100$, where X is conversion, $[A]^0$ and $[A]$ are inlet and outlet gas concentrations in ppm, respectively. The selectivity

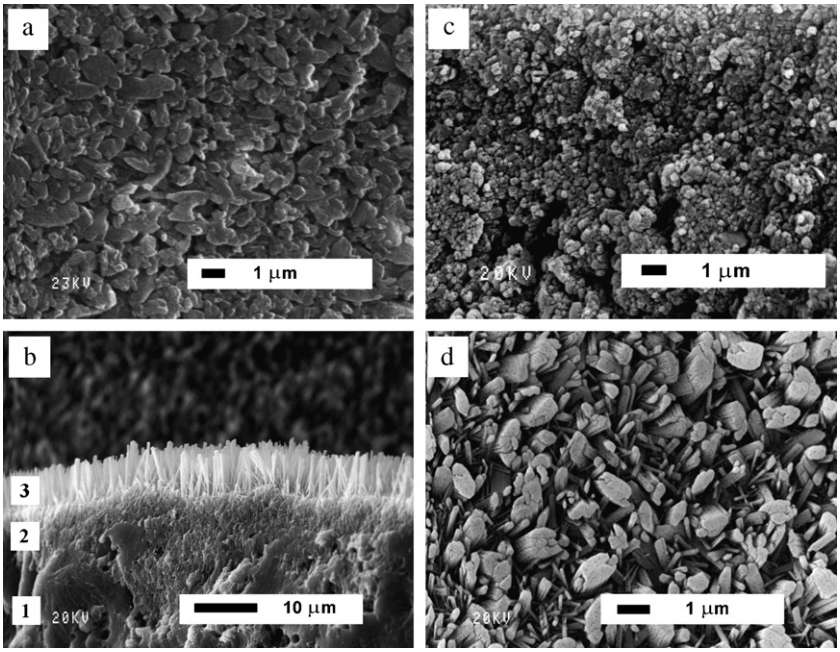

Fig. 1. Scanning electron microscopy (SEM) images of the zeolite monolith with hybrid properties (HM). (a) Cross-section which shows: (1) the cordierite support, (2) the particulated zeolite coating and (3) the secondary growth on the coating surface. (b) Close view of the particulated zone of the HM. (c) Top view of the washcoat surface before the hydrothermal treatment. (d) Top view of the surface secondary growth.

in the NO_x conversion due to the catalytic selective reduction was calculated as: $S_{NO_x} = \frac{X_{NO}}{X_{CH_4}} \times 100$.

Gaseous mixtures were analyzed before and after reaction with an on-line FTIR Thermo Mattson Genesis II equipped with a gas analysis cell for the NO, NO_2 and CH_4 quantification (N_2O was not detected).

3. Results and discussion

3.1. Microstructure of the monolith

After the washcoating, which was carried-out in two steps, the zeolite loading corresponded to a weight gain of 12.5 wt.% while after the hydrothermal treatment the weight gain was 21 wt.%, thus generating a total increment of 33.5 wt.%. Fig. 1a shows an upper view of the washcoated monolith (WM) before the hydrothermal treatment. Despite the fact that the zeolite particles present in the powder can reach a size of 15 μm [18], only small crystals with sizes below 1 μm can be observed at the surface of the washcoated monolith. This well-ordered small-crystals array could be originated by capillary forces during the drying process, in which the evaporation of the solvent generates a capillary drainage of the smaller particles from the inner film towards the surface.

The weight gained after the hydrothermal treatment suggest the generation of zeolite crystals growing from the aggregates deposited during the washcoating, which act as seeds. In Fig. 1b, the cross-section SEM picture shows the complex structure of the hybrid monolith (HM). At the bottom of the picture, the cordierite substrate shows its external macropores that give place to the rough interphase and the internal wall pores (in the 1–3 μm size range). Above the interphase, the zeolite aggregates deposited during the washcoating are observed (zone 2). These aggregates are partially stabilized by the porous structure of the cordierite surface. However, the microstructure of the particulated coating is more compact as compared to that obtained with conventional washcoating [18]. Fig. 1c shows a magnification in the cross-section of the particulated zone (zone 2 in Fig. 1b), where the aggregates and void spaces between them can be observed. This morphology is similar to that characteristic of the zeolite films obtained by washcoating, but with a higher intergrowth structure, formed during the hydrothermal treatment. The said intergrowth is more clearly seen in Fig. 2, in which a detail of the aggregates in the cross-section of HM is presented. The image lets us see a micro-rough surface of the aggregates due to the development of nanometric crystals and a merged aspect of the aggregates given by an intergrowth.

On the other hand, onto the merged aggregates (inside the monolith channels), vertically aligned crystals develop at the surface of the coating, which are produced by a secondary growth (Fig. 1b, zone 3). These prismatic crystals are 5 μm long and similar to those developed by a secondary growth performed on bare cordierite monoliths (SM) [15], albeit with a somewhat narrower

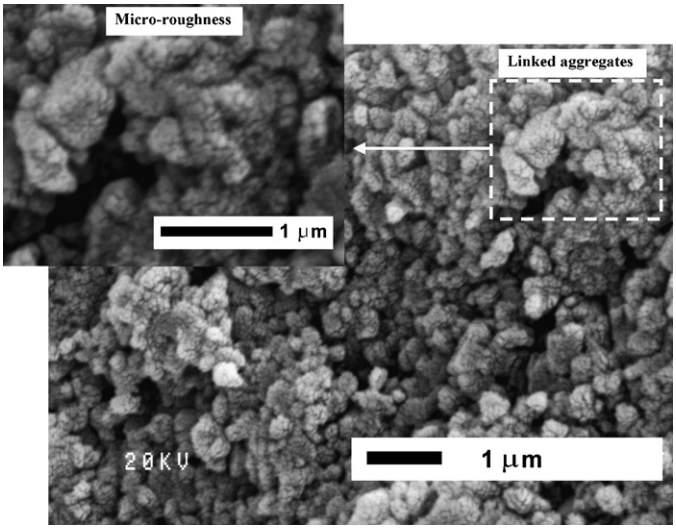

Fig. 2. Scanning electron microscopy (SEM). Close-up of the zeolite aggregates in the HM showing the linked aggregates and their surface micro-roughness, generated by the crystal growths during the hydrothermal treatment.

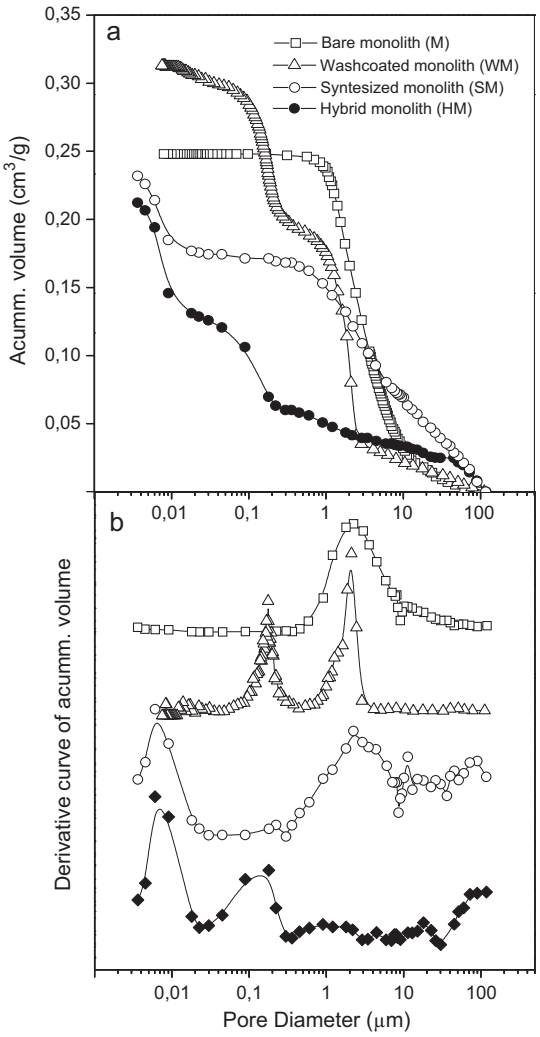

Fig. 3. Mercury intrusion porosimetry (MIP) profiles: (a) cumulative intrusion curves; (b) derivative of the respective cumulative curves. □ Bare cordierite monolith (M); Δ zeolite washcoated monolith (WM); ○ Synthesized zeolite monolith (SM); ● Hybrid zeolite monolith (HM).

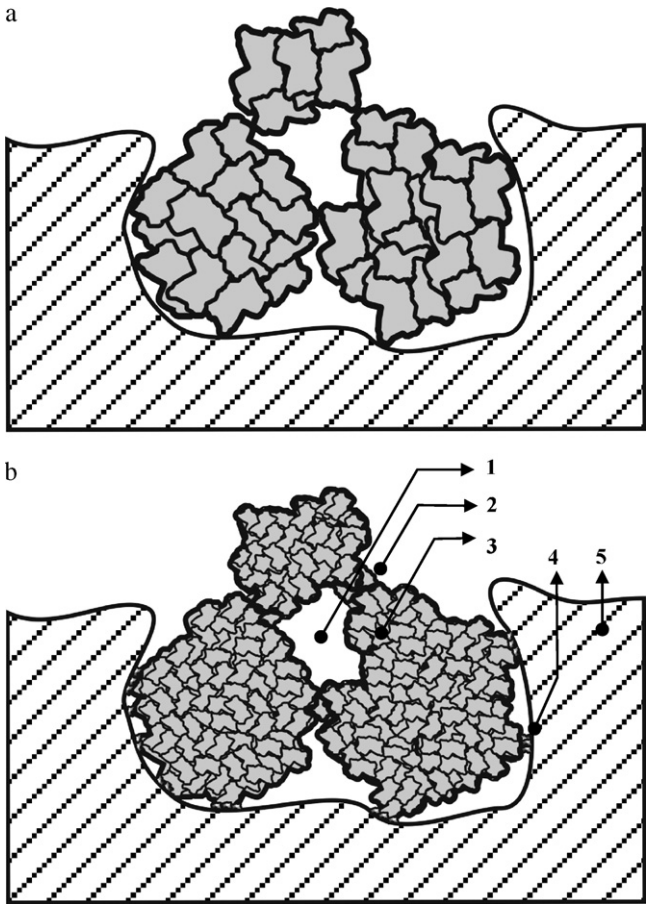

Fig. 4. Scheme of the zeolite aggregates in the particulated coating deposited inside of a cordierite pore. (a) Particles deposited by washcoating. (b) Particles in the HM after the hydrothermal treatment: (1) size reduction of the pores formed between aggregates; (2) increase in the number of contact points between aggregates (fusion); (3) development of surface micro-roughness due to the presence of small crystals; (4) new contact points with high interaction with the support; (5) cordierite support.

section. This similarity is originated by the presence of the well-ordered nanocrystal film that develops after the washcoating, as discussed above (see Fig. 1a). These small crystals behave as seeds giving place to the superficial growth observed in the hybrid coating. When viewed from the upper side (Fig. 1d), it can be observed that the small sized crystals (less than 1 μm) are arranged forming intercrystalline voids in the form of slits, generating a new porosity, similar to the one observed in the SM sample. However, in the present case the crystals grow 20–50 μm far from the cordierite support, indicating that the microstructure developed by these crystals is not strongly affected by the chemical characteristics of the support.

3.2. Porosity of the monolith

The micro-structural characteristics of the HM, evidenced by the SEM pictures, are strongly related to the porous structure analyzed by MIP and shown in Fig. 3a. In the same figure, the porosity profiles of the bare cordierite monolith (M), the washcoated monolith (WM), and the monolith with a secondary growth (SM) are also shown. The MIP profile of the bare monolith (M) shows a continuous increment of the intrusion volume, from the macropores range with a maximum at 2 μm, up to the zone of smaller pores near 0.5 μm. After that, no variations are observed. This behavior is due to the macroporosity of the cordierite support. On the other hand, when the monolith is covered by a mordenite washcoat, a lower intrusion volume is observed for the 0.5–2 μm range, due to the partial filling of the cordierite monolith pores with mordenite crystals. Besides, in the WM a bimodal distribution is developed due to the formation of another porous structure with porous sizes centered at 0.17 μm, fact that is clearly seen in the derivative curve (Fig. 3b). During the washcoating, the mordenite crystals are deposited in the form of aggregates, and the void spaces between the crystals originate the new kind of porosity observed.

In the case of the HM, a decrease in the pore volume of the cordierite structure takes place (Fig. 3a), which is more important than that observed for the WM. The MIP peak due to the inter-aggregates porosity is still present. However, this porosity presents a lower volume, the peak is wider, and shifted to smaller sizes (0.3–0.03, centered at 0.13 μm) if compared with the washcoated sample. These characteristics are indicative of a development of zeolite crystals between the aggregates during the hydrothermal treatment, fact that is in agreement with the previous SEM observations (Figs. 1 and 2).

Another feature of the HM sample is the formation of pores centered at 50 nm, similar to the one observed in the SM (Fig. 3). This kind of porosity can be safely attributed to the void spaces

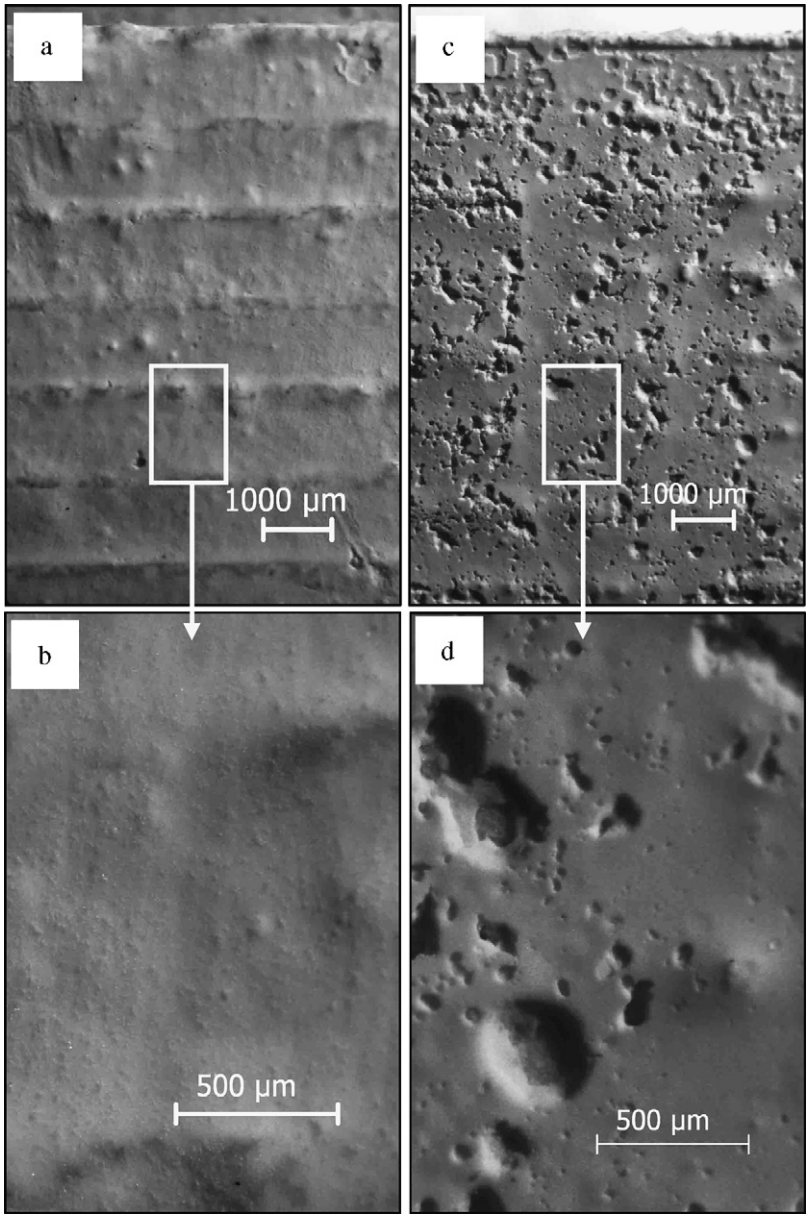

Fig. 5. Optical microscopic images of the samples after the ultrasonic adherence test (ultrasonic bath in water at 47 kHz and 130 W for 1 h at 25 °C). (a) The surface of the hybrid coating (HM) remains unchanged. (b) Close view of the surface in the HM that shows no damage. (c) The surface of the washcoat with silica binder suffers erosion. (d) Close view of the washcoat with silica binder at the surface, showing the crater-like holes caused by ultrasonic cavitation.

between the crystals grown on the surface of the particulated coating (see Fig. 1d). As said above, the HM presents a weak signal in the zone of the macropores centered at 2–3 μm, which are characteristic of the cordierite, probably due to a blockage produced by the intergrown mordenite aggregates and by a crystal growth inside the cordierite macropores. The intergrowth among the mordenite aggregates that takes place during the hydrothermal treatment has important implications in the pore size distribution of the coating. It is reasonable to think that the said intergrowth should also have an important effect on the adherence of the coating. In order to corroborate this point, adherence tests will be analyzed in the following section.

According to the above-discussed results, the picture of the aggregates in the HM could be represented as the scheme in Fig. 4. After the washcoating, the mordenite aggregates deposited on the cordierite macropores preserve their individuality, originating pores between them (Fig. 4a). After the hydrothermal treatment (Fig. 4b), a considerable amount of small crystals at the surface of the aggregates develops, which generates a micro-roughness (Fig. 2) and an intergrowth that bind the aggregates among them and probably also to the surface of the cordierite. This phenomenon decreases the inter-particle volume (Fig. 3a) and the size of the corresponding pores (Fig. 3b), but the macroporous structure of the washcoat is still preserved (Fig. 1). The aggregates present in the coating appear as a porous block in which the particles are strongly attached between them and with the support.

3.3. Mechanical stability

The incorporation of binders, e.g. colloidal silica or alumina, during the washcoating procedure is a usual practice aimed to increase the mechanical stability of the coating. It is claimed that the effect of the binders is to increase the number of contact points between washcoat particles, developing higher cohesive forces among them

[27]. The intergrowth between zeolite aggregates that develops in the HM could play the same role as the binders.

In order to evaluate the stability of the HM, it was subjected to an ultrasonic test (see Section 2). Prior to the stability test, the monolith was under reaction conditions during several hours and at temperatures between 400 °C and 600 °C. After the stability test, the hybrid coating (mass = 426 mg) suffered a weight loss of 4.4 wt.%. This weight loss is much lower than that produced in binderless mordenite-washcoated monoliths (13 wt.% [18]) that corroborates an increase in the adherence of the coating due to the existence of an intergrowth between mordenite aggregates caused by the hydrothermal treatment. However, the weight loss observed in the HM resulted slightly higher than that observed in the WM in which 3 wt.% of silica was used as binder [18]. In order to analyze this observation in depth, adherence tests were performed in cordierite plates obtained by cutting one-channel pieces of monolith covered by zeolite films which were deposited either by the combined method or by washcoating (in the latter case using 3 wt.% of a colloidal silica binder). Fig. 5 shows optical micrographs of these samples after the severe ultrasound treatment. It can be observed that the hybrid coating does not present damaged zones (see Fig. 5a) which is further corroborated with the magnification shown in Fig. 5b. On the contrary, for the sample obtained by washcoating with 3 wt.% of colloidal silica, a damaged aspect is observed after the ultrasound test (Fig. 5c). A crate-shaped erosion is produced by the ultrasonic cavitation, whose details are shown in Fig. 5d. Moreover, in some zones the film is totally detached.

The microscopic characterization clearly demonstrates that the coating in the HM gives place to a high adherence which is in turn higher than that observed for the binder-assisted washcoating procedure. Despite the fact that the weight loss of the HM sample expressed in wt.% was slightly higher, the microscopic analysis allowed us to conclude that the majority of the weight loss in the HM is not due to a loss of pieces of coating but probably to the detachment of material weakly adhered to the surface, which remained as an impurity after the hydrothermal treatment. A way to check this hypothesis is to record the weight loss of the HM in repeated ultrasonic tests. After a second treatment, the weight loss of the coating was 0.9 wt.% and after a third treatment, it was negligible (0.1 wt.%). These values together with the microscopic observations shown above demonstrate the high stability of the hybrid coating.

On the basis of what has been discussed it can be concluded that, besides yielding an intermediate structure between the washcoated monolith and the coating obtained for secondary synthesis, in the hybrid monolith a much better adherence is developed as compared with the binder-assisted washcoat (Fig. 5). The coating preserves part of the porosity obtained during the washcoating (Figs. 1 and 3) and the intergrowth of zeolite crystals (Fig. 2) plays the role of the binder, without introducing a different material in the system.

So far, we have shown the structural characteristics of the monolith; in the following sections we shall discuss their chemical and catalytic properties.

3.4. NO temperature-programmed desorption (NO-TPD)

In order to assess the catalytic behavior of the HM, indium was exchanged as an active ingredient for the SCR of NO_x reaction, which will be discussed in the final section. The question is how the new physicochemical characteristics developed in the hybrid coating affect the behavior of the indium exchanged species. We chose the NO-TPD technique for two reasons: the first one is that it provides a sensitive technique to characterize different indium species [28] and the second is that NO being the main reactive in the SCR reaction, it is important to assess its interaction with the catalytic surface.

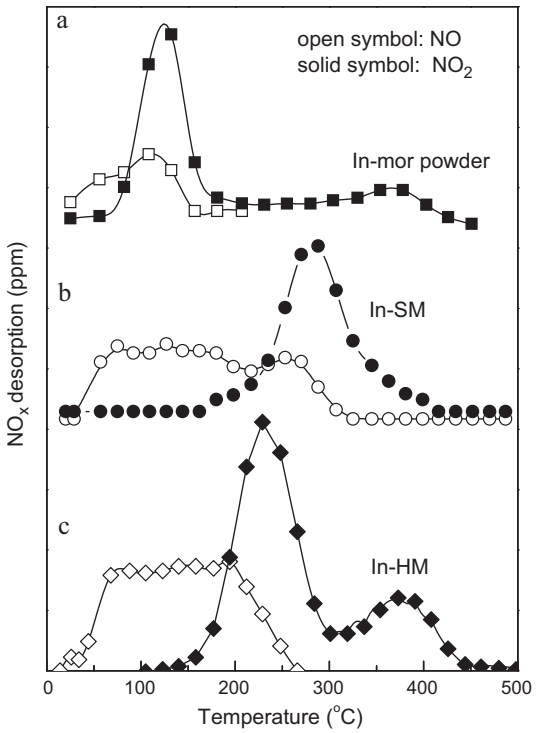

Fig. 6. Nitric oxide temperature-programmed desorption (NO-TPD) profiles. (a) In–mordenite powder catalyst. (b) Synthesized In–mordenite/monolith catalyst (In–SM). (c) Hybrid In–mordenite/monolith catalyst (In–HM). Open symbols correspond to NO signals and solid symbols correspond to NO_2 signals.

Fig. 6c shows the NO-TPD profile for the hybrid monolith in which indium has been incorporated by solid-state ion exchange (In–HM), showing a predominance of NO_2 desorption. The low-temperature NO_2 desorption signal (NO_2^L) can be attributed to the interaction of NO with exchanged InO^+ species, and the high-temperature NO_2 desorption (NO_2^H) to highly dispersed In_xO_y patches. The NO desorption can be assigned to the interaction with non-exchanged indium sesquioxide. This profile resembles that obtained with a powder sample (Fig. 6a) but with somewhat different desorption temperatures and bigger NO evolution, which extends from 100 °C to 250 °C. On the other hand, this latter signal is also similar to that observed for indium exchanged cordierite monolith with secondary synthesis (In–SM) as can be seen in Fig. 6b.

The addition of metal oxides done by impregnation followed by solid-state exchange, which is the method employed in this work, can result in different species distributions upon the porous structure of the solid support. In this vein, those indium precursors hosted in the cordierite pores placed in the inner zones of the monolith walls, after thermal treatment, will result in the formation of dispersed In_2O_3. The presence of this oxide which does not interact with zeolite crystals (placed inside the cordierite pores), originates the NO signal in the NO-TPD experiments. For this reason, the signal for the In–HM is similar to that developed in the In–SM, as can be seen in Fig. 6. The presence of indium in the support was also proved by EMPA analyses as we will show in next section.

The indium precursors hosted in the surface of zeolite agreggates, instead, are able to generate more dispersed oxides with a stronger interaction with the zeolite, originating, as said before, the NO_2^H peaks. Because these species are in the zeolite surface their magnitude is related to the structural characteristics of the particles. A relation between particle size and the proportion of indium species in their external surface was reported by Ogura et al. for

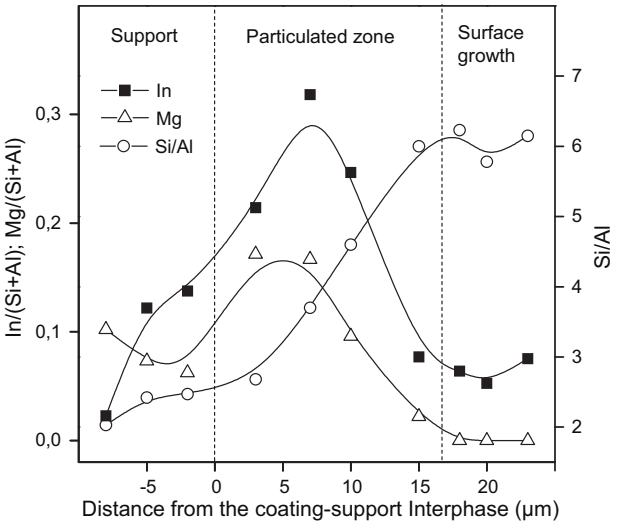

Fig. 7. Electron probe microanalysis (EPMA) profile of the indium-exchanged hybrid monolith (In–HM). Indium (■) and magnesium (△) contents relative to the (Si + Al) and Si/Al ratio (○), are plotted against coating thickness (the 0 μm value of the thickness correspond to the cordierite-coating interphase and the negative values are analysis points into the support).

In–ZSM5 catalysts [29]. Fig. 6 shows that the $NO_2{}^H$ signal is present in the form of a well-defined peak in the case of the In–HM, but it develops as a shoulder in the case of the In–SM, and as a weak signal in the powder. In the three cases, the desorption temperature is the same (370 °C). The higher intensity of $NO_2{}^H$ on In–HM could be due to the high proportion of small crystals developed in the aggregates (see Fig. 2), where impregnated indium precursors can accumulate, thus forming larger amounts of In_xO_y. The structural characteristics of the zeolite crystals may affect the behavior of In species during the impregnation and drying steps because during these processes, polynuclear cations $In[(OH)_2In]_n{}^{3+n}$ can be formed and deposited on the external surface of the crystals [30].

Furthermore, the In precursors that have access to the zeolite micropores can be exchanged as InO^+ species producing the $NO_2{}^L$ signals. Fig. 6 shows strong shifts of the $NO_2{}^L$ desorption temperature between the samples, most likely due to differences in diffusive restrictions in the coating. It was noted above that the SM monolith presents a more closed crystalline structure compared to HM monolith. Thus, the more compact the structure, the higher is the temperature needed for NO_2 desorption. As a matter of fact, the accessibility of the sites of the In–HM is intermediate between the powder and the In–SM.

Following, the composition of the indium-exchanged hybrid monolith is analyzed.

3.5. Elemental composition (EPMA)

Fig. 7 shows the composition profiles in a cross-section of the In–HM. It can be seen that the indium concentration passes through a maximum in the particulated zone. There is also an appreciable amount of indium inside the macropores of the cordierite, which is similar to that found on the surface of the coating.

On the other hand, the Si/Al ratio in the coating decreases from the outer surface towards the coating inside, reaching values close to those of the cordierite. The increase in aluminum from the interface can be caused by a partial dissolution of the substrate and by a differentiated incorporation of Al in the zeolite during the hydrothermal treatment. This implies that part of the aluminum is of the zeolite framework and part remains between the crystals. This latter assumption is supported by observing the magnesium profile. This element that can come only from the support, presents a maximum in the particulated zone.

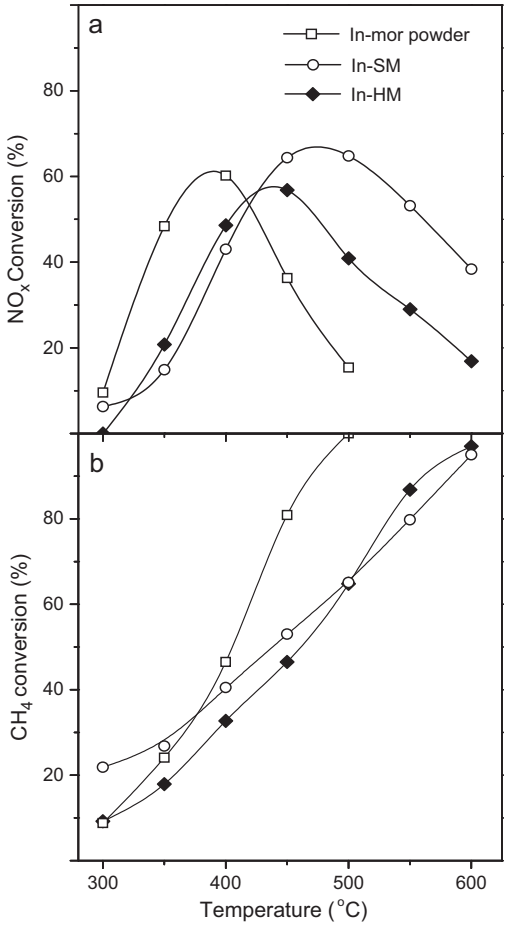

Fig. 8. Catalytic behavior of the indium-exchanged hybrid monolith reactor (In–HM) in the selective catalytic reduction (SCR) of NO_x with methane. For comparison In–zeolite powder and synthesized In–zeolite/monolith (In–SM) performances are included. (a) NO_x conversion curves; (b) CH_4 conversion curves. □ In–mordenite powder catalyst; ○ In–mordenite synthesized monolith (In–SM); ♦ In–mordenite hybrid monolith (In–HM). *Reaction conditions*: 1000 ppm NO, 1000 ppm CH_4, 10% O_2, 500 $cm^3\ min^{-1}\ g\ zeolite^{-1}$ total flow/zeolite loading ratio.

The distribution of indium in the coating is correlated with the NO-TPD profiles discussed in the previous section. The indium in the support (Fig. 7) is in the form of dispersed oxides (In_2O_3) which originate the NO desorption signal (Fig. 6c). Meanwhile, the porosity existing between aggregates leads to a high retention of indium precursors in this zone during the impregnation step, as can be seen in Fig. 7. After thermal activation exchanged (InO^+) species are formed into the zeolite micropores, but due to the high amount of precursors in this zone and the high external surface of the aggregates provided by their micro-roughness (see Fig. 2), a larger proportion of dispersed oxides in interaction with the zeolite (as In_xO_y) are also generated. These oxides are responsible for the higher $NO_2{}^H$ desorption signal as seen in the NO-TPD (Fig. 6c).

3.6. Catalytic performance

As demonstrated in previous sections, the combined procedure of preparing the catalytic zeolite coating causes the film to develop particular characteristics in stability, porosity, microstructure and chemical composition. It is reasonable to think that this may affect the catalytic performance of the system.

The curves for the NO_x and methane conversions obtained during the SCR of NO_x reaction over In–HM are depicted in Fig. 8. The

corresponding curves for In–SM and for the In–mordenite powder catalyst are included for comparison. The results show a promising behavior of the monolith reactor, using high spatial velocities.

Although the NO_x conversion for the In–HM is slightly lower as compared with that of the powder (Fig. 8a), it presents a wider activity window, which is intermediate between the behavior of the In–SM and the powder. Besides, the temperature necessary for the maximum NO_x conversion is located between those of the other two systems. These temperatures are 390 °C < 440 °C < 480 °C for the powder, In–HM and In–SM, respectively.

Not only the NO conversion important in the reaction under study but also the selectivity, which can be defined as the ratio between NO_x conversion and methane conversion (see Section 2). The selectivity is a measure of the amount of methane used as reductant to reach a given NO_x conversion. The maximum selectivity value possible in the reaction under study under the employed conditions is 2. The maximum selectivity values obtained were 1.98 (at 350 °C), 1.48 (at 400 °C) and 1.27 (at 450 °C) for the In–mordenite powder, In–HM and In–SM (the temperature of the maximum selectivity is indicated between brackets).

The differences observed in activity and selectivity are a function of the different distribution of In species developed. However, the morphological characteristics are also important, because they may pose limitations to the accessibility to the active sites. In this sense, the powder catalyst should have the most advantageous morphological conformation since all the aggregates are exposed to the gaseous flow. If the two monolithic catalysts are compared, in Fig. 8 it can be seen that the performances are similar, showing NO_x conversions in a similar temperature range. On the other hand, the selectivity of the hybrid sample is somewhat higher, which is due to the lower methane conversions at temperatures below 500 °C (Fig. 8b). The activity and selectivity results confirm that the In–HM catalyst has a good catalytic performance even at high spatial velocities.

4. Conclusions

A novel structured catalyst is obtained by combining washcoating and hydrothermal synthesis procedures. This system consists in a zeolite coating deposited on a cordierite monolith that has a porous microstructure similar to that obtained with the washcoat procedure, having an intercrystalline growth that greatly increases the adherence avoiding the use of a binder. It is demonstrated that the physicochemical characteristics and catalytic behavior of hybrid indium/zeolite monolith (In–HM) are intermediate between those obtained using either washcoating or hydrothermal secondary synthesis alone. The monolith showed high catalytic activity and selectivity for the SCR of NO_x at high spatial velocities.

Thus, it is concluded that this combined preparation method offers a new route for obtaining highly adherent and porous zeolitic structured catalysts without using a binder material. The obtained monolithic reactor can be used in demanding conditions, like those given in real environmental applications. Moreover, with this method, the porous properties of the final catalyst could be tuned by adjusting synthesis conditions such as synthesis time and reactives concentration during the hydrothermal treatment.

Acknowledgments

The authors are grateful for the financial support received from Universidad Nacional del Litoral, CONICET and ANPCyT. Thanks are also given to Elsa Grimaldi for the English language editing.

References

[1] R.M. Heck, S. Gulati, R.J. Farrauto, Chem. Eng. J. 82 (2001) 149.
[2] J.S. Howitt, Corning Glass Works, Advances in automotive catalysts supports. in: Crucq, Frennet (Eds.), Catalysis and Automotive Pollution Control. Elsevier Science, 1987, p. 301.
[3] H. Choi, S.W. Ham, I. Nam, Y.G. Kim, Ind. Eng. Chem. Res. 35 (1) (1996) 106.
[4] Z.S. Rak, H.J. Veringa, React. Kinet. Catal. Lett. 60 (2) (1997) 303.
[5] E.I. Basaldella, A. Kikot, C.E. Quincoces, M.G. González, Mater. Lett. 51 (2001) 289.
[6] L. Li, J. Chen, S. Zhang, N. Guan, M. Richter, J. Catal. 228 (2004) 12.
[7] A.E.W. Beers, T.A. Nijhuis, F. Kapteijn, J.A. Moulijn, Micropor. Mesopor. Mater. 48 (2001) 279.
[8] A.E.W. Beers, T.A. Nijhuis, N. Aalders, F. Kapteijn, J.A. Moulijn, Appl. Catal. A: Gen. 243 (2003) 237.
[9] O. Ohrman, J. Hedlund, J. Sterte, Appl. Catal. A: Gen. 270 (2004) 193.
[10] M.A. Ulla, E. Miro, R. Mallada, J. Coronas, J. Santamaría, Chem. Commun. (2004) 528.
[11] G.B.F. Seijger, A. van den Berg, R. Riva, K. Krishna, H.P.A. Calis, H. van Bekkum, C.M. van den Bleek, Appl. Catal. A: Gen. 236 (2002) 187.
[12] C.D. Madhusoodana, R.N. Das, Y. Kameshima, A. Yasumori, K. Okada, Micropor. Mesopor. Mater. 46 (2001) 249.
[13] S. Candamo, P. Frontera, F. Crea, R. Aiello, Top. Catal. 30–31 (2004) 369.
[14] Y. Han, H.S. Zeng, N. Guan, Catal. Commun. 3 (2002) 221.
[15] J.M. Zamaro, M.A. Ulla, E. Miró, Appl. Catal. A: Gen. 314 (2006) 101.
[16] M.A. Ulla, R. Mallada, L.B. Gutierrez, L. Casado, J.P. Bortolozzi, E.E. Miro, J. Santamaría, Catal. Today 133–135 (2008) 42.
[17] M.A. Ercoli, J.M. Zamaro, C.E. Quincoces, E.E. Miró, M.G. González, Chem. Eng. Commun. 195 (2008) 417.
[18] J.M. Zamaro, M.A. Ulla, E.E. Miró, Chem. Eng. J. 106 (2005) 25.
[19] A.V. Boix, J.M. Zamaro, E.A. Lombardo, E.E. Miró, Appl. Catal. B: Environ. 46 (2003) 121.
[20] A.V. Boix, S.G. Aspromonte, E.E. Miró, Appl. Catal. A: Gen. 341 (2008) 26.
[21] K. Masuda, K. Shinoda, T. Kato, K. Tsujimura, Appl. Catal. B: Environ. 15 (1998) 29.
[22] A. Obuchi, I. Kaneko, J. Uchisawa, A. Ohi, A. Ogata, G.R. Bamwenda, S. Kushiyama, Appl. Catal. B: Environ. 19 (1998) 127.
[23] V. Tomasic, Z. Gomzi, Chem. Biochem. Eng. Q 15 (3) (2001) 109.
[24] A.V. Boix, E.E. Miró, E.A. Lombardo, R. Mariscal, J.L.G. Fierro, Appl. Catal. A: Gen. 276 (12) (2004) 197.
[25] A. Eleta, P. Navarro, L. Costa, M. Montes, Micropor. Mesopor. Mater. 123 (2009) 113.
[26] L. Lisi, R. Pirone, G. Russo, V. Stanzione, Chem. Eng. J. 154 (1–3) (2009) 341.
[27] T.A. Nijhuis, A.E.W. Beers, T. Vergunst, I. Hoek, F. Kapteijn, J.A. Moulijn, Catal. Rev. 43 (4) (2001) 345.
[28] J.M. Zamaro, H.P. Decolatti, L.B. Gutierrez, A. Martínez, G.A. Fuentes, in preparation.
[29] M. Ogura, T. Ohsaki, E. Kikuchi, Micropor. Mesopor. Mater. 21 (1998) 533.
[30] E.E. Miró, L. Gutiérrez, J.M. Ramallo-López, F.G. Requejo, J. Catal. 188 (1999) 375.